

# Effects of Surface Roughness on Large-Volume CdZnTe Nuclear Radiation Detectors and Removal of Surface Damage by Chemical Etching

G.W. Wright<sup>a</sup>, G. Camarda<sup>b</sup>, E. Kakuno<sup>b</sup>, L. Li<sup>c</sup>, F. Lu<sup>c</sup>, C. Lee<sup>c</sup>, A. Burger<sup>d</sup>, J. Trombka<sup>e</sup>,  
P. Siddons<sup>b</sup>, R. B. James<sup>a</sup>

<sup>a</sup>Nonproliferation and National Security Department,  
Brookhaven National Laboratory, Upton, NY 11973

<sup>b</sup>National Synchrotron Light Source,  
Brookhaven National Laboratory, Upton, NY 11973

<sup>c</sup>Yinnel Tech, Inc., South Bend, IN 46619

<sup>d</sup>Center for Photonic Materials and Devices, Physics Department,  
Fisk University, Nashville, TN 37211

<sup>e</sup>Laboratory for Extraterrestrial Physics, Goddard Space Flight Center,  
Greenbelt, MD 20771

## ABSTRACT

This study investigates the effectiveness of chemical etchants to remove surface damage caused by mechanical polishing during the fabrication of Cd<sub>0.9</sub>Zn<sub>0.1</sub>Te (CZT) nuclear radiation detectors. We evaluate different planar CZT devices fabricated from the same CZT crystals. All detectors used electroless Au for the metal contacts. Different polishing particle sizes ranging from 22.1- $\mu$ m SiC to 0.05- $\mu$ m alumina were used, which caused different degrees of surface roughness. Current-voltage measurements and detector testing were used to characterize the effects of surface roughness and etching on the material and detector properties.

## 1. INTRODUCTION

Previous studies reported the effects of the choice of chemical etchant on the device performance of CZT.<sup>1-4</sup> Using high-pressure Bridgman (HPB) CZT material, it was shown that the choice of etchant could have either a deleterious or beneficial effect on device performance. In general, the etchant that produced the smoothest surface morphology as measured by AFM usually resulted in the fabrication of planar devices exhibiting higher resistivity, better ohmicity, and better energy resolution for the 32-keV photopeak of <sup>133</sup>Ba. In a subsequent paper the authors demonstrated that the choice of metal deposition technique could also have a major influence on device performance.<sup>5</sup> In Ref. (5), it was demonstrated that gold contacts deposited by thermal evaporation gave better device performance, exhibiting higher apparent resistivity, better ohmicity, and less noise. Studies on effects of different etchants<sup>2</sup> and metal deposition<sup>5</sup> techniques showed that the photoluminescence data had a one-to-one correspondence between the FWHM of the donor bound exciton peak and the energy resolution of the detector. These reports underscored the importance of surface damage and sub-surface crystallinity on the metal contact-CZT interface, noise in the devices, and detector quality.

Modified vertical Bridgman (MVB) and horizontal Bridgman (MHB) techniques led to a new class of high resistivity CZT materials with increased yield and supply of large-volume single crystals greater than 100 cm<sup>3</sup>.<sup>6</sup> These materials exhibited different metal contact/ CZT interface behavior compared to HPB-grown crystals. Wright et al. demonstrated

that for a large-volume MVB {111} oriented single CZT crystal, the metal/CZT interface behavior and corresponding device performance were dependent upon the choice of etchant and the surface orientation.<sup>4</sup> Ref. (4) employed the same battery of different etchants; however, slightly different outcomes were deduced with most chemical etchants yielding device performances that were asymmetric and contingent upon the surface orientation (e.g., (111)A vs. (111)B). This paper found that for {111} oriented MVB CZT material the best overall planar device performance, which was symmetric for both surfaces (111)A and (111)B, was produced with a 2%-Br<sub>2</sub> in 20% lactic acid in ethylene glycol solution. An unexpected result was also demonstrated that a fine polish with 0.05- $\mu\text{m}$  alumina and no chemical etchant yielded the best overall response for the (111)A Cd-terminated surface, however, for the (111)B surface, the worst overall response was observed. This result strongly suggested that both surface morphology and surface stoichiometry play roles in controlling the metal/CZT interface behavior and the resulting device performance.

In this paper, we control the surface morphology by using different polishing grits of 22.1- $\mu\text{m}$  and 0.05- $\mu\text{m}$ . The I-V behavior and device performance for planar CZT detectors fabricated with and without 2% (v/v) Br<sub>2</sub>/Methanol etchant are compared. Each fabricated device was passivated by immersion in 10% (w/w) NH<sub>4</sub>F/H<sub>2</sub>O<sub>2</sub> in 25 mL of water.<sup>7,8</sup> The I-V and device performance results are reported before and after surface passivation.

## 2. EXPERIMENT

In our experimental approach we fabricate four CZT planar devices from the same 10 x 10 x 6.5 mm<sup>3</sup> CZT crystal using four different processes described as follows: In process I all six surfaces of the CZT crystal are roughly polished using only 22.1- $\mu\text{m}$  grit SiC polishing paper, **RP**. The CZT crystal was not subsequently etched. Immediately following polishing, Au metal was deposited on two opposing planar surfaces via the electroless method. In process II all six surfaces of the CZT crystal were fine polished using 0.05- $\mu\text{m}$  alumina grit, **FP**. The CZT crystal was not subsequently etched. Immediately following polishing, Au metal was deposited via the electroless Au method. In process III all six surfaces of the CZT crystal were roughly polished using 22.1- $\mu\text{m}$  grit SiC polishing paper. The CZT crystal is subsequently etched in 2% Br<sub>2</sub>/methanol; and immediately following etching, Au metal was deposited via the electroless Au method, **RFBM**. Lastly, in process IV all six surfaces were finely polished using 0.05- $\mu\text{m}$  Alumina. The CZT crystal was subsequently etched in 2% Br<sub>2</sub>/methanol, and immediately following etching, Au metal was deposited via the electroless Au method, **FPBM**. Current-voltage measurements and detector tests were completed. After this testing the fabricated detectors were subsequently immersed, without protection of the electroless Au contacts, in 10% (w/w) NH<sub>4</sub>F/H<sub>2</sub>O<sub>2</sub> in 25 mL of water for 10 minutes to study the effects of this surface passivation technique.

Results from the 4 different experiments are reported and discussed. Case I involves the comparison of fine polishing (0.05  $\mu\text{m}$ ) versus rough polishing (22.1  $\mu\text{m}$ ) without any etchants, **FRP**. Case II is the comparison of fine polishing versus rough polish with out any etchant after passivation in NH<sub>4</sub>F/H<sub>2</sub>O<sub>2</sub> aqueous solution, **FRP+NF**. Case III studies the comparison of fine polishing with Br<sub>2</sub>/methanol etchant versus rough polishing with Br<sub>2</sub>/methanol etchant, **FRPBM**. Case IV investigates the comparison of fine polishing with Br<sub>2</sub>/methanol etchant versus rough polishing with Br<sub>2</sub>/methanol etchant after passivation in NH<sub>4</sub>F/H<sub>2</sub>O<sub>2</sub> aqueous solution, **FRPBM+NF**.

All detector performance measurements were taken at the same bias of 500 V with the exception of 200 V for the rough polished sample. The shaping time was 0.5  $\mu\text{s}$ , coarse gain was at 500, fine gain was 0.5, and the acquisition time was 250 seconds. The distance to the source was kept constant at 1.0 cm, and the detector was shielded from the source via a beryllium window.

### 3. RESULTS AND DISCUSSION

#### 3.1 Current-Voltage Results

Fig. 1 demonstrates the effects of rough polishing vs. fine polishing, Case I, on the current-voltage behavior of planar CZT detectors. Fig. 2 demonstrates the effects of rough polishing vs. fine polishing, Case II, on the current-voltage behavior after immersion of the electroless Au planar CZT detector in  $\text{NH}_4\text{F}/\text{H}_2\text{O}_2$ . Rough polishing produced extremely leaky CZT detectors that exhibited injecting contacts with a maximum current in the  $\mu\text{A}$  range for a bias voltage at  $\pm 500$  V. The current-voltage response of the fine polished planar CZT detector showed slightly blocking contacts at low voltages with a maximum current in the  $10\text{nA}$  range at  $\pm 500$  V. Immersion of the unprotected electroless Au contacts in  $\text{NH}_4\text{F}/\text{H}_2\text{O}_2$  solution resulted in a significant reduction in the leakage current for the rough-polished detector, while the fine-polished fabricated planar CZT detector had a slightly higher leakage current as shown in Fig. 2. The  $\text{NH}_4\text{F}/\text{H}_2\text{O}_2$  immersed rough-polished sample had a higher leakage current at negative bias with greater noise in its response.

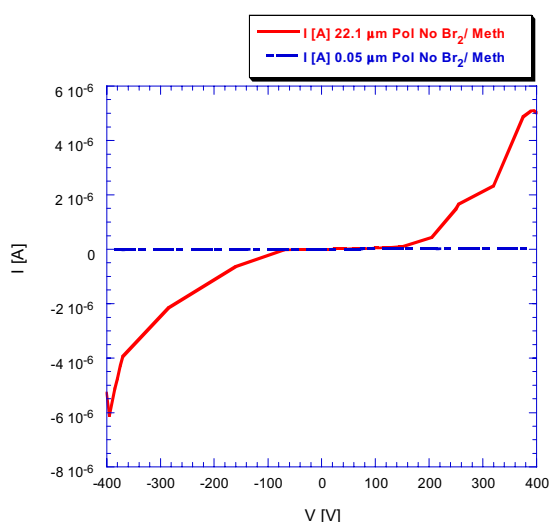


**Figure 1** Case I: Current-Voltage measurements for 22.1- $\mu\text{m}$  SiC vs. 0.05- $\mu\text{m}$  Alumina polish and no etchant. **Before** passivation in  $\text{NH}_4\text{F}/\text{H}_2\text{O}_2$  solution.

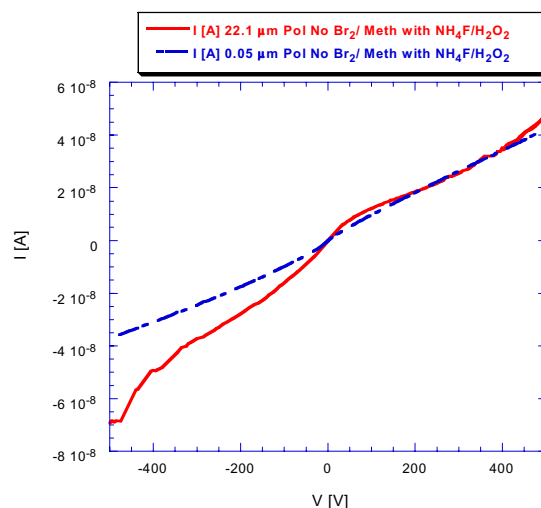


**Figure 2** Case II: Current-Voltage measurements for 22.1- $\mu\text{m}$  SiC vs. 0.05- $\mu\text{m}$  Alumina polishing and no etchant. **After** passivation in  $\text{NH}_4\text{F}/\text{H}_2\text{O}_2$  solution.

Figures 3 and 4 demonstrate the effect of  $\text{Br}_2$ /methanol on the current-voltage response of the rough versus fine polished planar detectors. The rough-polished detector with  $\text{Br}_2$ /methanol etchant exhibited lower leakage current with a maximum current in the  $10\text{-nA}$  range at  $\pm 500$  V, whereas the fine-polished detector with  $\text{Br}_2$ /methanol etchant exhibited higher leakage current with a maximum current in the  $100\text{-nA}$  range at  $\pm 500$  V. The introduction of the etchant process produced detectors with better ohmic contacts albeit with higher leakage current for some surfaces. In Figure 4 both the rough and fine polished detectors with 2%  $\text{Br}_2$ /methanol etchant planar CZT detectors were immersed in  $\text{NH}_4\text{F}/\text{H}_2\text{O}_2$  with their electroless Au contacts unprotected from the  $\text{NH}_4\text{F}/\text{H}_2\text{O}_2$  solution. The immersion in  $\text{NH}_4\text{F}/\text{H}_2\text{O}_2$  solution reduced the linearity of the current-voltage response for both the fine and rough polished with  $\text{Br}_2$ /methanol etchant CZT detectors. The current-voltage curves demonstrated slightly injecting contacts, as shown in Fig. 4. The leakage current was approximately the same for positive bias range, while in the negative bias range, the leakage current was slightly higher for the fine-polished detector with  $\text{Br}_2$ /methanol etching after immersion in  $\text{NH}_4\text{F}/\text{H}_2\text{O}_2$  solution. The rough-polished detector with  $\text{Br}_2$ /methanol after immersion in  $\text{NH}_4\text{F}/\text{H}_2\text{O}_2$  solution exhibited a noticeable change in the shape of the current-voltage curve, indicating charge injection at both bias polarities. The leakage current, although still in the  $10\text{-nA}$  range at negative bias was 3 times as high after immersion in the  $\text{NH}_4\text{F}/\text{H}_2\text{O}_2$  solution, while in the positive bias range, the leakage current had increased to a maximum of about  $100\text{ nA}$  at  $500\text{ V}$ .

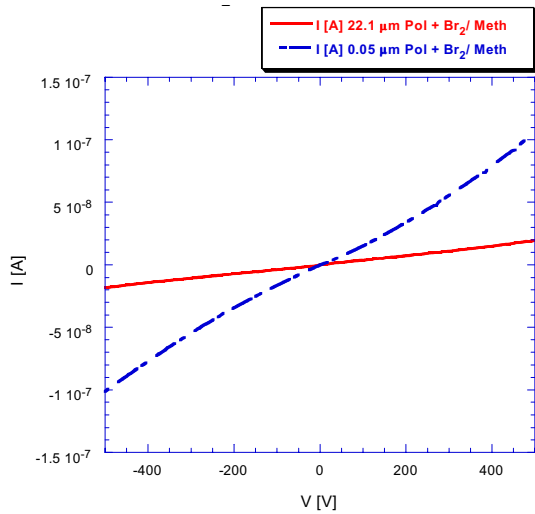


**Figure 3** Case III: Current-Voltage measurements with 22.1- $\mu\text{m}$  SiC and 0.05- $\mu\text{m}$  Alumina polishing and 2%  $\text{Br}_2/\text{Methanol}$  etchant. **Before** passivation in  $\text{NH}_4\text{F}/\text{H}_2\text{O}_2$  solution.

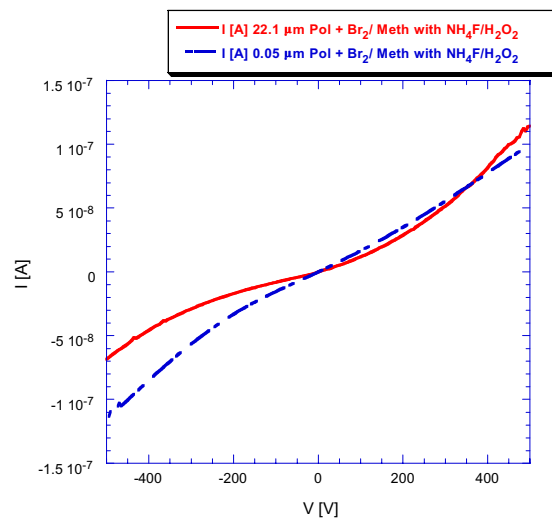


**Figure 4** Case IV: Current-Voltage measurements with 22.1- $\mu\text{m}$  SiC and 0.05- $\mu\text{m}$  Alumina polishing and 2%  $\text{Br}_2/\text{Methanol}$  etchant. **After** passivation in  $\text{NH}_4\text{F}/\text{H}_2\text{O}_2$  solution.

### 3.2 Device Performance Results with $^{241}\text{Am}$

Figs. 5 and 6 demonstrate the effects on device performance of rough polishing with 22.1- $\mu\text{m}$  SiC versus fine polishing with 0.05  $\mu\text{m}$  without any chemical etchant. Results are shown before and after immersion in the  $\text{NH}_4\text{F}/\text{H}_2\text{O}_2$  passivation solution, respectively. Rough polishing without any etchant results in a broad continuum of noise without any ability to resolve counts in the photo-peaks. Fine polishing without any etching does exhibit the ability to resolve the low energy x-ray in to photo-peaks, although the efficiency of this device is lower as evidenced by a lower number of registered counts. Immersing the entire sample with unprotected electroless Au contacts into  $\text{NH}_4\text{F}/\text{H}_2\text{O}_2$  solution resulted in the ability of the roughly polished sample to resolve the 59.6-keV peak for  $^{241}\text{Am}$ , while in the fine-polished sample case without any etchant, we observed an increase in the charge collection efficiency, as evidenced by an increase in the number of counts. However, no improvement in the energy resolution was observed.

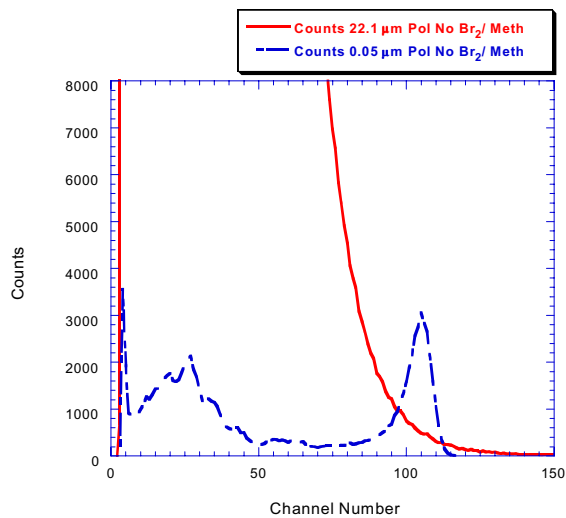


**Figure 5** Case I:  $^{241}\text{Am}$  Spectrum with 22.1- $\mu\text{m}$  SiC and 0.05- $\mu\text{m}$  Alumina polishing and no etchant. **Before** passivation in  $\text{NH}_4\text{F}/\text{H}_2\text{O}_2$  solution.

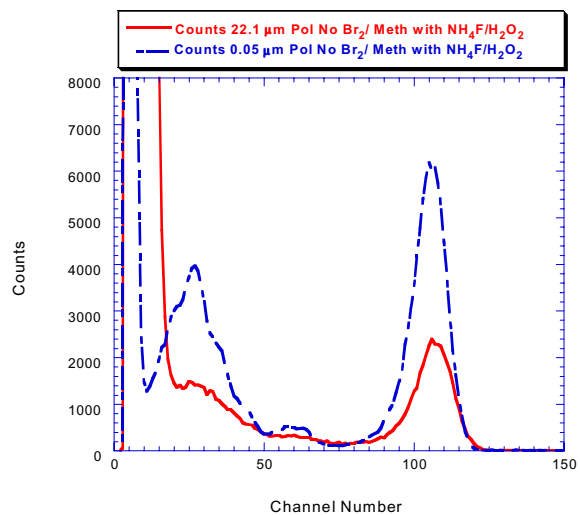


**Figure 6** Case II  $^{241}\text{Am}$  Spectrum with 22.1- $\mu\text{m}$  SiC and 0.05- $\mu\text{m}$  Alumina polishing and no etchant. **After** passivation in  $\text{NH}_4\text{F}/\text{H}_2\text{O}_2$  solution.

Figs. 7 and 8 demonstrate the effects on device performance of 2% Br<sub>2</sub>/methanol ability to remove the surface damage from rough-polished versus fine-polished detectors. The subsequent step of Br<sub>2</sub>/methanol after mechanical polishing resulted in the rough-polished detector obtaining the ability to resolve the registered counts into photo-peaks with an improved peak-to-valley ratio greater than the fine polished with Br<sub>2</sub>/methanol etchant. The addition of Br<sub>2</sub>/methanol enhanced the charge collection efficiency of both the rough and fine polished fabricated detectors, as evidenced by the increase in registered counts. However, the trend established in Fig. 6 regarding the ability of NH<sub>4</sub>F/H<sub>2</sub>O<sub>2</sub> to improve electroless Au planar fabricated device's charge collection efficiency did not occur for the rough-polished detector with Br<sub>2</sub>/methanol etchant due to a significant increase in noise with corresponding degradation in the energy resolution, as shown in Fig. 8. Furthermore the current-voltage behavior, shown in Fig. 4, had changed from slightly blocking to slightly injecting, indicating the metal/CZT interface had changed after immersion of the rough-polished detector with Br<sub>2</sub>/methanol etching into the NH<sub>4</sub>F/H<sub>2</sub>O<sub>2</sub> solution.

The trend was re-established in the fine-polished sample with Br<sub>2</sub>/methanol etching after subsequent immersion in NH<sub>4</sub>F/H<sub>2</sub>O<sub>2</sub>, even though the fine-polished detector with Br<sub>2</sub>/methanol etching before immersion in NH<sub>4</sub>F/H<sub>2</sub>O<sub>2</sub> did not perform as well as the rough polished detector with Br<sub>2</sub>/methanol etchant. The fine-polished sample with Br<sub>2</sub>/methanol etching after immersion in NH<sub>4</sub>F/H<sub>2</sub>O<sub>2</sub> exhibited the best device performance out of all the device fabrication schemes.

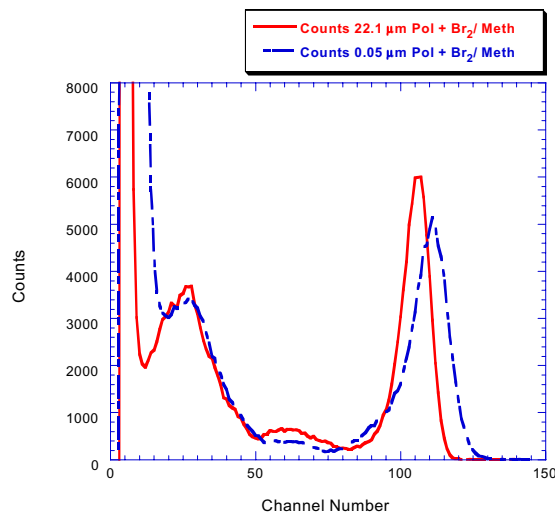


**Figure 7** Case III: <sup>241</sup>Am Spectrum with 22.1-µm SiC and 0.05-µm Alumina polishing with 2% Br<sub>2</sub>/Methanol etchant. **Before** passivation in NH<sub>4</sub>F/H<sub>2</sub>O<sub>2</sub> solution.

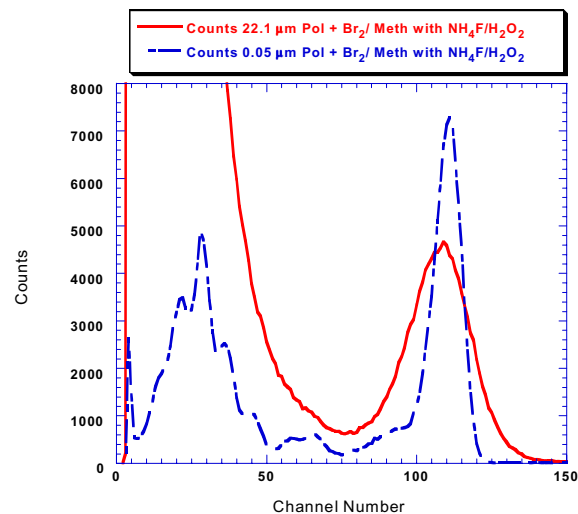


**Figure 8** Case IV: <sup>241</sup>Am Spectrum with 22.1-µm SiC and 0.05-µm Alumina polish with 2% Br<sub>2</sub>/Methanol etchant. **After** passivation in NH<sub>4</sub>F/H<sub>2</sub>O<sub>2</sub> solution.

### 3.3 Summary of Results

The results of this study are summarized in Table I and Table II below. Here, the current-voltage results are compared to device performance results. The contact area for the planar devices fabricated from the same CZT crystal was 10 x 10 mm<sup>2</sup> with the thickness of the various devices between 6 mm to 6.5 mm. A slight reduction in the thickness of the sample was due to the series of mechanical polishing processes conducted in device fabrication. The total counts in Table II are the summation of resolved counts registered above the low energy noise.

The term ohmicity in Table I is defined as the standard deviation error from a linear fit of the equation  $I = mV + I_0$  through the experimental data points. Where  $I$  is the current,  $m$  is the slope of the  $I$ - $V$  curve,  $V$  is the voltage, and  $I_0$  is the intercept of  $I$  when  $V$  is zero.

**Table I.** Comparison of Surface Roughness Effects on Current-Voltage Measurements.

Fabrication Cases		Resistivity	Ohmicity	Leakage Current @ 500 V in nA	Leakage Current @ -500 V in nA
Polished	22.1 $\mu\text{m}$	$1.54 \times 10^8$	0.944	5,008	-5,280
	0.05 $\mu\text{m}$	$2.81 \times 10^{10}$	0.994	33.3	-23.0
Polished w/ $\text{NH}_4\text{F}/\text{H}_2\text{O}_2$	22.1 $\mu\text{m}$	$1.54 \times 10^{10}$	0.992	47.8	-69.3
	0.05 $\mu\text{m}$	$2.02 \times 10^{10}$	0.998	42.2	-37.1
$\text{Br}_2/\text{Methanol}$	22.1 $\mu\text{m}$	$4.54 \times 10^{10}$	0.999	19.4	-18.3
	0.05 $\mu\text{m}$	$8.66 \times 10^9$	0.998	107.9	-101.2
$\text{Br}_2/\text{Methanol}$ w/ $\text{NH}_4\text{F}/\text{H}_2\text{O}_2$	22.1 $\mu\text{m}$	$1.08 \times 10^{10}$	0.976	114.7	-68.3
	0.05 $\mu\text{m}$	$8.40 \times 10^9$	0.996	99.4	-116.4

**Table II.** Comparison of Surface Roughness Effects on CZT Planar Device Performance with  $^{241}\text{Am}$  Response

Fabrication Cases		FWHM @ 59.6 KeV	Peak-to-Valley @ 59.6 KeV	Photo-Peak Counts @ 59.6 KeV	Total Counts $^{241}\text{Am}$ Spectrum
Polished	22.1 $\mu\text{m}$	N/A	N/A	N/A	N/A
	0.05 $\mu\text{m}$	9.2	14.1	37,873	92,749
Polished w/ $\text{NH}_4\text{F}/\text{H}_2\text{O}_2$	22.1 $\mu\text{m}$	15.0	15.7	40,289	76,492
	0.05 $\mu\text{m}$	12.1	55.7	90,140	182,420
$\text{Br}_2/\text{Methanol}$	22.1 $\mu\text{m}$	10.4	26.4	75,628	176,410
	0.05 $\mu\text{m}$	13.4	24.5	87,094	163,350
$\text{Br}_2/\text{Methanol}$ w/ $\text{NH}_4\text{F}/\text{H}_2\text{O}_2$	22.1 $\mu\text{m}$	24.5	7.5	122,020	N/A
	0.05 $\mu\text{m}$	10.5	41.8	95,308	199,100

Table I shows that the resistivity increased for the rough-polished sample without any etchant after immersion in  $\text{NH}_4\text{F}/\text{H}_2\text{O}_2$  solution. The resistivity decreased for the fine-polished detector without any etchant after immersion in  $\text{NH}_4\text{F}/\text{H}_2\text{O}_2$  solution. Even with the lowering of resistivity after immersion of the fine-polished detector without etchant in  $\text{NH}_4\text{F}/\text{H}_2\text{O}_2$  solution, Table II shows that the fine-polished detector without etchant immersed in  $\text{NH}_4\text{F}/\text{H}_2\text{O}_2$  solution produced the highest peak-to-valley ratio at 59.6 keV and the second highest number of total registered counts. This result suggests that having a smooth surface morphology that is close to bulk stoichiometry will improve CZT planar detector performance.

The highest ohmicity shown in Table I is obtained with the 22.1- $\mu\text{m}$  grit with chemical etching and with the fine-polished detector with etchant, although the fine-polished detector exhibited lower resistivity and higher leakage current. After immersion of the rough-polished detector with etchant and fine-polished detector with etchant in  $\text{NH}_4\text{F}/\text{H}_2\text{O}_2$  solution, the ohmicity of both detectors went down with comparably higher leakage currents. However, even with the increase in leakage current and decrease in ohmic behavior, the fine-polished detector with etchant produced the best device performance after immersion in  $\text{NH}_4\text{F}/\text{H}_2\text{O}_2$  solution, as demonstrated in Table II. The fine-polished detector with etchant after immersion in  $\text{NH}_4\text{F}/\text{H}_2\text{O}_2$  solution fabrication process registered the greatest amount of counts in the 59.6 keV photopeak with the second highest peak-to-valley ratio and the second best energy resolution at 59.6 keV.

## CONCLUSIONS

The benefits of fine polishing or smooth surface morphology underneath the metal contact are evidenced in Fig 5, where without any etchant the planar CZT device was still able to resolve registered events into photo-peaks, including the low energy x-rays from  $^{241}\text{Am}$ . The addition of 2%  $\text{Br}_2/\text{methanol}$  etchant into the fabrication process resulted in enhanced device sensitivity for both the rough and fine polished sample, as evidenced by an increase in the number of

registered events. This increased device sensitivity came at the expense of reduced energy resolution due to an increase in leakage current resulting from the nonstoichiometric surface left after Br<sub>2</sub>/methanol etching. The increase in leakage current due to Br<sub>2</sub>/methanol etching could be minimized by optimizing the etching time and concentration of Br<sub>2</sub>, so that the smoothest surface morphology with the least amount of change in surface stoichiometry is produced.

The effects of increased leakage current were mitigated in three cases after immersion of the unprotected electroless Au contacts in the NH<sub>4</sub>F/H<sub>2</sub>O<sub>2</sub> solution: rough polished with no etchant, fine polished with no etchant, and fine polished with 2% Br<sub>2</sub>/methanol etchant. After immersion of the unprotected electroless Au contacts in the NH<sub>4</sub>F/H<sub>2</sub>O<sub>2</sub> solution, the device performance of both the fine polished and fine polish with etchant planar CZT devices resulted in a significant increase in counts with the fine polished with Br<sub>2</sub>/methanol etchant detector acquiring both enhanced sensitivity and a significant increase in energy resolution, as evidenced in Fig. 8 by the good resolution of the low-energy x-ray peaks of <sup>241</sup>Am and the improved peak-to-valley ratio of the <sup>241</sup>Am photo-peaks.

However, the improvement in device performance cannot solely be attributed to a decrease in the leakage current, where higher leakage current was achieved after immersion in NH<sub>4</sub>F/H<sub>2</sub>O<sub>2</sub>. For all other cases, the fine polishing without etchant and the fine polishing with etchant after immersion in NH<sub>4</sub>F/H<sub>2</sub>O<sub>2</sub> produced planar CZT devices with slightly higher leakage current. Even though the device had a slightly higher leakage current, the charge collection efficiency of the device had increased as evidenced by the increase in registered events. This finding seems to suggest that the NH<sub>4</sub>F/H<sub>2</sub>O<sub>2</sub> solution is not only affecting the lateral surfaces, but may also affect the metal/CZT semiconductor interface in a beneficial way by either increasing the uniformity of the E-field and/or by lowering the surface recombination velocity underneath the metal contact.

The increase in leakage current after immersion in NH<sub>4</sub>F/H<sub>2</sub>O<sub>2</sub> is opposite of the finding previously reported by Wright et al. However, the finding is parallel to what was reported by Prettyman et al. The difference in the two authors work is that Wright et al protected the Au contact using Humiseal, while Prettyman et al used unprotected sputtered gold contacts.

At first glance the increase in leakage current after immersion in NH<sub>4</sub>F/H<sub>2</sub>O<sub>2</sub> is inconsistent with the findings previously reported by Wright et al. However, the finding agrees qualitatively with the report by Prettyman et al.<sup>9</sup> The difference in the experiments performed by the two authors is that Wright et al. protected the Au contact using Humiseal, while Prettyman et al. used unprotected sputtered metal gold contacts. In both cases the NH<sub>4</sub>F/H<sub>2</sub>O<sub>2</sub> solution could potentially alter the interface between the metal and the CZT semiconductor interface by attacking the adhesion of the Au contact. In the original Wright et al. paper, the metal/semiconductor interface was protected, which prevents the NH<sub>4</sub>F/H<sub>2</sub>O<sub>2</sub> solution from attacking the contact. In the work reported here the electroless Au contact was not protected, which is similar to the unprotected sputtered Au contacts studied by Prettyman et al.<sup>9</sup> The key to enhanced device performance with the unprotected electroless Au contacts after immersion in NH<sub>4</sub>F/H<sub>2</sub>O<sub>2</sub> may be due to the method of metal deposition and its resistance to the NH<sub>4</sub>F/H<sub>2</sub>O<sub>2</sub> solution. The electroless Au deposition process is facilitated by a chemical reaction at the interface between the metal and CZT substrate. This reaction layer acts as a barrier or a chemical intermediate that could be converted to a dielectric film after NH<sub>4</sub>F/H<sub>2</sub>O<sub>2</sub> immersion, depending on the porosity of the Au and interfacial layer between the electroless deposited Au and CZT interface. Thermally evaporated and sputtered Au use a physical process to deposit the metal, thus there is not an interfacial reacted layer of uniform chemical composition. Furthermore, the NH<sub>4</sub>F/H<sub>2</sub>O<sub>2</sub> solution may diffuse differently around or through the edges of the metal contacts deposited by thermal evaporation or sputtering process.

This work shows that fine polishing to obtain the smoothest surface morphology as possible and subsequent chemical etching to remove surface damage are necessary in order to produce the best performance from planar CZT detectors made from MVB-grown CZT material. This work also demonstrates that immersion of unprotected electroless Au contacts in NH<sub>4</sub>F/H<sub>2</sub>O<sub>2</sub> aqueous solution can result in increased charge collection efficiency of planar CZT nuclear radiation detectors. The effects of surface orientation and etchants on surface stoichiometry have not yet been fully optimized, and further study is needed to elucidate the best fabrication process for this material.

## FUTURE WORK

Future studies will be initiated to hone in on whether the  $\text{NH}_4\text{F}/\text{H}_2\text{O}_2$  is actually undercutting the Au electrode and chemically altering the interface underneath the electrode. Also, tests to understand the effects of unprotected thermally evaporated or sputtered Au contact versus protected metal-CZT semiconductor interface on the same crystal will be completed. Finally, the use of a guard ring structure to eliminate edge and surface leakage current will be implemented, so that we can ascertain how much of the increase in leakage current is due to charge injection at the contact versus surface leakage current.

## ACKNOWLEDGEMENTS

The authors thank Dr. Peter Siddons for his fruitful discussions and use of his laboratory facilities. This work was supported by Brookhaven National Laboratory's Directed Research and Development (LDRD) program.

## REFERENCES

1. H. Chen, S. U. Egarievwe, Z. Hu, J. Tong, D. T. Shi, G. H. Wu, K. T. Chen, M. A. George, W. E. Collins, A. Burger, R. B. James, "Study of Gamma-Ray Detector Performance of Cadmium Zinc Telluride Crystals Treated by Different Etchants", *SPIE Conference on Hard X-Ray/Gamma-Ray and Neutron Optic, Sensors, and Applications*, Vol. **2859**, 254, (1996).
2. H. Chen, J. Tong, Z. Hu, D. T. Shi, G. H. Wu, K.-T. Chen, M. A. George, W. E. Collins, A. Burger, R. B. James, C. M. Stahle, "Low Temperature Photoluminescence of Detector Grade  $\text{Cd}_{1-x}\text{Zn}_x\text{Te}$  Crystals Treated by Different Chemical Etchants," *J. Appl. Phys.*, **80(6)**, 3509, (1996).
3. Y. Cui, G. W. Wright, X. Ma, K. Chattopadhyay, R. B. James and A. Burger "DC Photoconductivity Study of Semi-Insulating  $\text{Cd}_{1-x}\text{Zn}_x\text{Te}$  Crystals", *Journal of Electronic Materials*, Vol. **30(6)**, 774-778, (2001).
4. G. Wright, Y. Cui, U. N. Roy, C. Barnett, K. Reed, A. Burger, F. Lu, L. Li, and R. B. James, "The Effects of Chemical Etching on the Charge Collection Efficiency of  $\{111\}$  Oriented  $\text{Cd}_{0.9}\text{Zn}_{0.1}\text{Te}$  Nuclear Radiation Detectors," *IEEE Transactions on Nuclear Science*, Vol. **49(5)**, 2521-2525, (2002).
5. A. Burger, H. Chen, J. Tong, D. Shi, M. A. George, K-T Chen, W. E. Collins, R. B. James, C. M. Stahle, and L. M. Bartlett, "Investigation of Electrical Contacts for  $\text{Cd}_{1-x}\text{Zn}_x\text{Te}$  Nuclear Radiation Detectors" *IEEE Transactions on Nuclear Science*, Vol. **44(3)**, 934-935, (1997).
6. L. Li, F. Lu, K. Shah, M. Squillante, L. Cirinano, W. Yao, R. W. Olsen, P. Luke, Y. Nemirovsky, A. Burger, G. Wright and R. B. James, "A New Method for Growing Detector-Grade Cadmium Zinc Telluride Crystals," *IEEE Nuclear Science Symposium Record*, Vol. **4**, 2396, (2002).
7. G. W. Wright, D. A. Chinn, B. A. Brunett, M. A. Mescher, J. Lund, R. Olsen, F. P. Doty, T. E. Schlesinger, R. B. James, K. Chattopadhyay, R. Wingfield, A. Burger, "Exploratory Search for Improved Oxidizing Agents Used in the Reduction of Surface Leakage Currents of  $\text{Cd}_{1-x}\text{Zn}_x\text{Te}$  Radiation Detectors," *SPIE Proceedings on Hard X-ray, Gamma Ray, and Neutron Detector Physics*, Proc. SPIE Vol. **3768**, 481-485, (1999).
8. G.W. Wright, R.B James, D.A. Chinn, B.A. Brunett, R. Olsen, J. Van Scyoc, M. Clift, A. Burger, K. Chattopadhyay, D. Shi and R. Wingfield, "Evaluation of  $\text{NH}_4\text{F}/\text{H}_2\text{O}_2$  effectiveness as a surface passivation agent for  $\text{Cd}_{1-x}\text{Zn}_x\text{Te}$  crystals", *Optical Science, Engineering, and Instrumentation Symposium*, Proc. SPIE Vol. **4141**, 324-335, (2000)
9. T.H. Prettyman, F. P. Ameduri, A. Burger, J. C. Gregory, M. A. Hoffbauer, P. R. Majerus, D. B. Reisenfeld, S. A. Soldner, Cs. Szeles, "Effects of Surfaces on the Performance of CdZnTe Detectors," *SPIE Proceedings on Hard X-ray, Gamma Ray, and Neutron Detector Physics*, Vol. **4507**, 23-31, (2001).